

Oxidative Dehydrogenation of the 2-Aminomethylpyridine (EDTA) Ruthenium (III) Complex

Henrique E. Toma and Maumi Tsurumaki

Instituto de Química, Universidade de São Paulo,
Caixa Postal 20780, São Paulo, SP, Brasil.

Received: October, 30, 1989

A desidrogenação oxidativa do ligante 2-aminometilpiridina (ampy) coordenado ao complexo (EDTA)Ru(III) foi investigada com base em medidas de voltametria cíclica, espectroeletroquímica e cinética "stopped-flow", em solução aquosa. O mecanismo de reação é consistente com a desprotonação do ligante ampy ($pK_a = 7.48$), seguida de uma etapa de transferência monoelétrica reversível. A espécie intermediária produzida nesta etapa passa por um processo de transferência eletrônica induzida pelo metal, com $k = 227 \text{ s}^{-1}$, convertendo-se no complexo correspondente de 2-iminometilpiridina.

The oxidative dehydrogenation of the 2-aminomethylpyridine (ampy) ligand coordinated to the (EDTA)Ru(III) complex was investigated based on cyclic voltammetry, spectroelectrochemistry and stopped-flow kinetic measurements in aqueous solution. The reaction mechanism is consistent with the deprotonation of the ampy ligand ($pK_a = 7.48$), followed by a reversible one-electron transfer step. The intermediate species generated at this step undergoes a metal-induced electron transfer process, with $k = 227 \text{ s}^{-1}$, converting into the corresponding 2-iminomethylpyridine complex.

Key words: oxidative dehydrogenation, EDTA-ruthenium(III) complex, aminomethylpyridine.

Introduction

Transition metal complexes containing amine ligands can undergo oxidative dehydrogenation reactions, yielding the corresponding imine products.¹⁻⁸ These reactions are of special interest since they involve metal-induced electron transfer processes⁹ of great relevance in catalysis and in bioinorganic chemistry¹⁰. Mechanisms based on the activation of the amine ligand by the metal ion in a high oxidation state have been proposed in these systems; however, the electron transfer process, which may involve two electron transfer⁴ or successive one electron transfer steps³, is not completely understood. In order to improve the understanding of the mechanisms of the dehydrogenation reactions, we carried out a detailed spectroelectrochemical and kinetic study on the (2-aminomethylpyridine) (EDTA) ruthenium (III) complex (EDTA = ethylenediaminetetraacetate ion) in aqueous solution.

Materials and Methods

Ruthenium trichloride, sodium trifluoroacetate (NaTFA) and 2-aminomethylpyridine (ampy) were supplied from Aldrich. The complex $[\text{Ru}(\text{HEDTA})(\text{H}_2\text{O})].3\text{H}_2\text{O}$ was prepared by the method of Mukaida *et al.*¹¹. Anal. calcd for $\text{RuC}_{10}\text{H}_{21}\text{N}_2\text{O}_{12}$: C, 26.0; H, 4.6; N, 6.0. Found: C, 26.0; H, 3.8; N, 6.0. The $[\text{Ru}^{\text{II}}(\text{EDTA})(\text{H}_2\text{O})]^{2-}$ complex was generated in solution, by reducing the $[\text{Ru}^{\text{III}}(\text{EDTA})(\text{H}_2\text{O})]^-$ ion electrochemically, or with zinc amalgam, under an argon atmosphere.

The $[\text{Ru}(\text{H}_2\text{EDTA})(\text{impy})].2\text{H}_2\text{O}$ (impy = 2-iminomethylpyridine) complex was prepared by mixing 1 mmol

of $[\text{Ru}(\text{HEDTA})(\text{H}_2\text{O})].3\text{H}_2\text{O}$ with 1 mmol of the 2-aminomethylpyridine (ampy) ligand, previously dissolved in 25 ml of water, in the presence of air. The deep red solution was concentrated to approximately 5 ml on a water bath and kept overnight at room temperature. The red crystalline material was collected on a filter and washed with ethanol. Yield 70%. Anal. calcd for $\text{RuC}_{16}\text{H}_{24}\text{N}_4\text{O}_{10}$: C, 36.0; H, 4.5; N, 10.5. Found: C, 36.0; H, 4.2; N, 10.5. The complex was diamagnetic. The infrared spectra exhibited characteristic H_2EDTA peaks at 1715 (s), 1420 (m) (COOH); 1570 (s), 1395 (s) cm^{-1} (COORu); and impy peaks at 1600 (s) (C=N), 1520 (w), 1495 (m), 1460 (m) (ring vibrational modes); 1400 (m), 1315 (w), 1300 (m), 1280 (m) (composite ring-H, C-C, C-N def. modes) and 1020 (m) cm^{-1} (ring breath mode) (s = strong, m = medium and w = weak intensity).

Cyclic voltammetry was carried out with a Princeton Applied Research (PAR) instrument, consisting of a model 173 potentiostat and a model 175 universal programmer. A gold disk electrode was employed for the measurements, using a conventional Luggin capillary arrangement with a Ag/AgCl reference electrode in 1.0 M KCl solution ($E^\circ = 0.222 \text{ V vs. SHE}$). A platinum wire was used as the auxiliary electrode.

The electronic spectra of the complexes were recorded on a model 8451-A Hewlett-Packard diode-array spectrophotometer. For the spectroelectrochemical measurements, the PAR 173 potentiostat was used in parallel with the HP-8451-A spectrophotometer. A three electrode sys-

tem was designed for a rectangular quartz cell of 0.020 cm internal optical path length. A gold minigrad was used as a transparent working electrode, in the presence of a small Ag/AgCl reference electrode and a platinum auxiliary electrode. All the measurements were performed at 25 °C under semi-infinite diffusion conditions.

The kinetics of the oxidative dehydrogenation reactions were carried out with a Durrum model D-110 stopped-flow apparatus, equipped with a Kel-F flow system. The data were obtained under pseudo-first order conditions at 25 °C, $I = 0.10$ M NaTFA in the presence of a high excess of the reactants over the ruthenium complex.

Results and Discussion

Solutions of $[\text{Ru}^{\text{III}}(\text{HEDTA})(\text{H}_2\text{O})]$ are pale yellow, exhibiting absorption bands at 284 nm ($\epsilon = 2800 \text{ M}^{-1} \text{ cm}^{-1}$) and 350 nm (680). The complex undergoes two successive acid-base equilibria in aqueous solution¹², corresponding to the deprotonation of the uncoordinated carboxylic group ($\text{p}K_{\text{a}} = 2.37$) and to the deprotonation of the coordinated water molecule ($\text{p}K_{\text{a}} = 7.63$). In the range of pH from 3 to 7, the $[\text{Ru}^{\text{III}}(\text{EDTA})(\text{H}_2\text{O})]^-$ complex is the major species. This ion exhibits an unusual fast kinetic behavior with respect to substitution reactions. The second order rate constants span the range $30 - 20,000 \text{ M}^{-1} \text{ s}^{-1}$, depending on the nature of the attacking ligands. The mechanism involved is typically associative¹².

In the presence of ampy, the $[\text{Ru}^{\text{III}}(\text{EDTA})(\text{H}_2\text{O})]^-$ complex yields a deep red product. If the reaction is carried out under an argon atmosphere, two strong absorption bands appear in the visible region, around 390 and 515 nm, as shown in Figure 1. Exploratory kinetic experiments using the stopped flow technique (Figure 1.A), indicated that the species absorbing at these two wavelengths are formed in parallel, with essentially the same rate constant, i.e., $k_{\text{obsd}} = 1.45$ and 1.40 s^{-1} , respectively, at 25 °C, $[\text{ampy}] = 0.050 \text{ M}$, $\text{pH} = 8.60$.

If the reaction is carried out in the presence of air, the electronic spectrum of the resulting solution coincides with that of the $[\text{Ru}^{\text{II}}(\text{EDTA})(\text{impy})]^{2-}$ product isolated in pure form, exhibiting a strong absorption at 514 nm ($\epsilon = 7.5 \times 10^3 \text{ M}^{-1} \text{ cm}^{-1}$), and a less intense band at 360 nm ($\epsilon = 4.8 \times 10^3 \text{ M}^{-1} \text{ cm}^{-1}$). These bands can be ascribed to metal-to-ligand charge-transfer transitions in the Ru(II)-diimine chromophore, by analogy to related examples from the literature¹³.

The reduced $[\text{Ru}^{\text{II}}(\text{EDTA})(\text{H}_2\text{O})]^{2-}$ complex reacts with ampy, yielding the orange-yellow $[\text{Ru}^{\text{II}}(\text{EDTA})(\text{ampy})]^{2-}$ product ($\lambda_{\text{max}} = 390 \text{ nm}$, $\epsilon = 6.0 \times 10^3 \text{ M}^{-1} \text{ cm}^{-1}$). In the presence of air, this species converts into the red $[\text{Ru}^{\text{II}}(\text{EDTA})(\text{impy})]^{2-}$ complex. A quantitative study of the amino-to-imino conversion was carried out spectroelectrochemically, as illustrated in Figure 2.

The $[\text{Ru}^{\text{II}}(\text{EDTA})(\text{ampy})]^{2-}$ complex is stable at negative potentials and can be readily identified by its characteristic Ru(II)-to-py $d_{\pi} - p_{\pi^*}$ charge transfer band at 390 nm. As the applied potential approaches 0.28 V vs SHE, the formation of the $[\text{Ru}^{\text{II}}(\text{EDTA})(\text{impy})]^{2-}$ product can be detected by the absorption bands at 514 and 360 nm, as shown in Figure 2A. At more positive potentials, the imine complex is oxidized to the corresponding Ru(III) species ($E^{\circ} = 0.57 \text{ V}$ vs SHE). By comparing the elec-

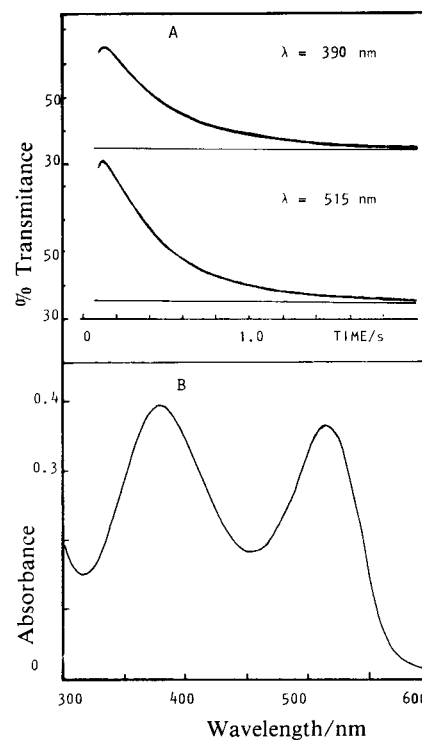


Figure 1. (A) Stopped-flow traces for the kinetics of reaction of $[\text{Ru}^{\text{III}}(\text{EDTA})(\text{H}_2\text{O})]^-$ ($5 \times 10^{-5} \text{ M}$) with ampy (0.050 M), 25 °C, $\mu = 0.10 \text{ M}$ NaTFA, $\text{pH} 8.60$, $\text{Na}_2\text{B}_4\text{O}_7/\text{H}_3\text{BO}_3$ buffer, 0.010 M ; (B) diode-array absorption spectrum of the reaction mixture measured after 1 s.

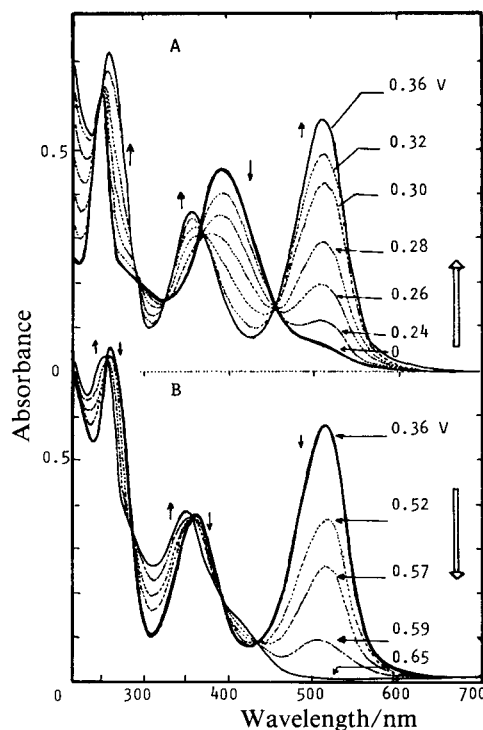
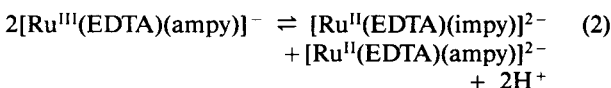
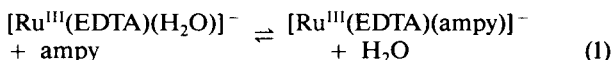


Figure 2. Spectroelectrochemical behavior of the $[\text{Ru}^{\text{II}}(\text{EDTA})(\text{ampy})]^{2-}$ complex ($3 \times 10^{-3} \text{ M}$), $\text{pH} 4.7$ (acetate buffer 0.05 M , $\text{KCl} 0.10 \text{ M}$, 25 °C, starting potential = 0 V; showing (A) the formation and (B) the oxidation of the corresponding impy product.

tronic spectrum of Figure 1.B, with those superimposed on Figure 2.A for the $[\text{Ru}^{\text{II}}(\text{EDTA})(\text{ampy})]^{2-}$ and $[\text{Ru}^{\text{II}}(\text{EDTA})(\text{impy})]^{2-}$ complexes, one can deduce that the reaction of the $[\text{Ru}^{\text{III}}(\text{EDTA})(\text{H}_2\text{O})]^-$ ion with ampy, under an argon atmosphere, leads to a 1:1 mixture of these two species, as expressed by equations (1) and (2):



The kinetic constants for the reaction of $[\text{Ru}^{\text{III}}(\text{EDTA})(\text{H}_2\text{O})]^-$ with ampy were of first order, in contrast to the second order behavior expected for reaction (2). On the other hand, the observed rate constants measured at pH 8.60, exhibited a linear dependence on the concentration of the ampy ligand. Therefore, at this pH, the rates of formation of the imine product are determined by the substitution reaction (1). According to Matsubara and Creutz¹² the reactivity of the $[\text{Ru}^{\text{III}}(\text{EDTA})(\text{H}_2\text{O})]^-$ complex decreases rapidly above pH 8, due to the deprotonation of the coordinated water molecule¹². Unfortunately, the kinetics can not be investigated below pH 8, since the rates are limited by the protonation of the free ampy ligand ($\text{p}K_{\text{a}} = 8.62$)¹⁴.

Cyclic voltammograms of the $[\text{Ru}^{\text{II}}(\text{EDTA})(\text{ampy})]^{2-}$ and $[\text{Ru}^{\text{II}}(\text{EDTA})(\text{impy})]^{2-}$ complexes are shown in Figure 3. Starting from the $[\text{Ru}^{\text{II}}(\text{EDTA})(\text{ampy})]^{2-}$ complex, at 0 V, a reversible redox wave (1) was observed with $E^{\circ} = 0.27\text{V}$ vs SHE (Fig. 3.A), assigned to the Ru(III)/(II) redox couple. This wave is followed by a second peak (2) at 0.41 V which is better seen at high potential scan rates (Figure 3.B), suggesting a transient species. At low potential scan rates, the redox wave (3) becomes well defined. This wave coincides with that for the $[(\text{EDTA})(\text{impy})\text{Ru}(\text{III})/(\text{II})]$ redox couple, with $E^{\circ} = 0.57\text{V}$, as shown in Figure 3.C.

According to the cyclic voltammograms of Figure 3.B the formation of the imine product is preceded by a transient species, responsible for the anodic peak (2). In order to elucidate the electron transfer process, we carried out a series of stopped-flow kinetic experiments starting from the $[\text{Ru}^{\text{II}}(\text{EDTA})(\text{ampy})]^{2-}$ complex and reacting with the hexacyanoferrate(III) ion. The OH^- concentration was kept constant using acetate or hydrogen phosphate buffers. An excess of the hexacyanoferrate (II) complex was also employed in the experiments, in order to ensure pseudo-first order conditions. All the experiments were carried out in triplicate, under an argon atmosphere. The reproducibility of the observed rate constants was higher than 5%.

The stopped-flow experiments showed a very rapid absorbance decay at 390 nm, near the mixing time of the equipment (1 ms), followed by the rise of the absorption band at 514 nm, corresponding to the formation of the $[\text{Ru}^{\text{II}}(\text{EDTA})(\text{impy})]^{2-}$ product. The kinetics monitored at 514 nm, exhibited a pseudo-first order behavior, yielding the observed rate constants shown in Table 1. The highest pH value was limited to 8, because in more alkaline solutions the $[\text{Ru}^{\text{II}}(\text{EDTA})(\text{impy})]$ complex is also ox-

idized by the hexacyanoferrate(III) ion precluding the observation of the absorption band at 514 nm.

The first rapid reaction was ascribed to the outer-sphere electron transfer between the $[\text{Ru}^{\text{II}}(\text{EDTA})(\text{ampy})]^{2-}$ complex and the hexacyanoferrate(III) ions. The reaction is practically quantitative, with a driving force of 150mV.

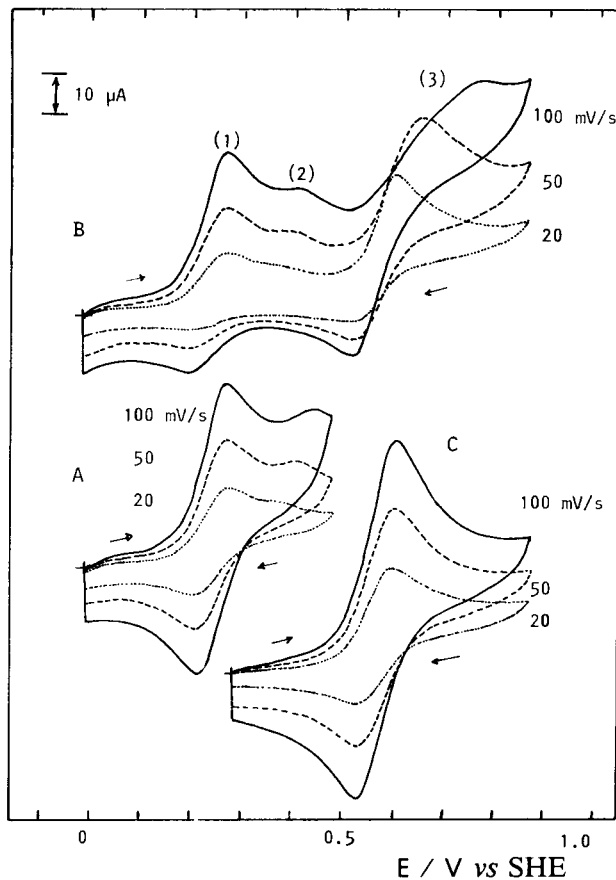
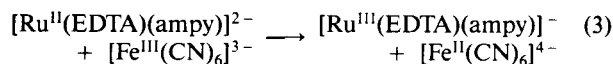


Figure 3. (A, B) Cyclic voltammograms of the $[\text{Ru}^{\text{II}}(\text{EDTA})(\text{ampy})]^{2-}$ complex ($3 \times 10^{-3}\text{M}$), and (C) of the $[\text{Ru}^{\text{II}}(\text{EDTA})(\text{impy})]^{2-}$ complex ($5 \times 10^{-3}\text{M}$) at several potential scan rates, pH 4.5 (acetate buffer 0.05 M), KCl 0.10 M, 25 °C.

The pseudo-first order rate constants shown in Table 1 refer to the formation of the $[\text{Ru}^{\text{II}}(\text{EDTA})(\text{impy})]^{2-}$ complex, and exhibit a non-linear increase on the concentrations of $[\text{OH}^-]$ and $[\text{Fe}^{\text{III}}(\text{CN})_6]^{3-}$ ions, and an inverse dependence on the concentration of the $[\text{Fe}^{\text{II}}(\text{CN})_6]^{4-}$ ion. This type of behavior can be rationalized in terms of a mechanism involving the deprotonation of the coordinated ampy ligand, followed by reversible electron transfer leading to an intermediate complex which undergoes internal electron transfer to generate the $[\text{Ru}^{\text{II}}(\text{EDTA})(\text{impy})]^{2-}$ product. The proposed mechanism can be seen in Figure 4:

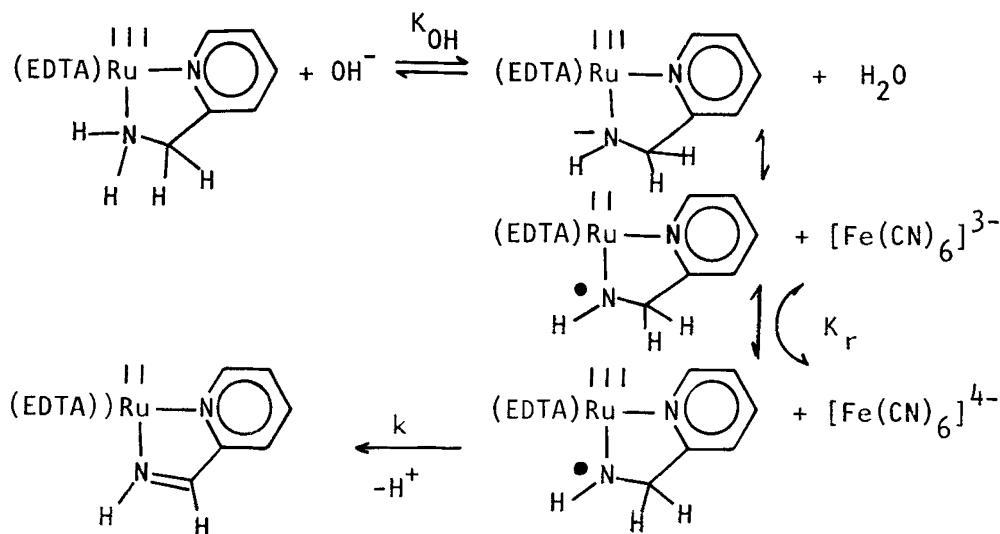


Figure 4. Mechanism proposed for the oxidative dehydrogenation of the coordinated 2-aminomethylpyridine ligand in the $[\text{Ru}^{\text{III}}(\text{EDTA})(\text{ampy})]^-$ complex.

Table 1. Observed rate constants for the oxidative dehydrogenation of the $[\text{Ru}^{\text{III}}(\text{EDTA})(\text{ampy})]^-$ complex.

Exp	$[\text{Fe}(\text{CN})_6]^{3-}$ (M)	$[\text{OH}^-]$ (M)	$[\text{Fe}(\text{CN})_6]^{4-}$ (M)	k_{obsd} (s^{-1})
1	2.50×10^{-4}	5.88×10^{-10}	2.50×10^{-4}	4.7×10^{-1}
2	2.50×10^{-4}	3.00×10^{-9}	2.50×10^{-4}	2.3
3	2.50×10^{-4}	6.00×10^{-9}	2.50×10^{-4}	3.7
4	2.50×10^{-4}	1.30×10^{-7}	2.50×10^{-4}	7.2×10
5	2.50×10^{-4}	1.60×10^{-7}	2.50×10^{-4}	7.1×10
6	5.00×10^{-4}	7.08×10^{-8}	2.50×10^{-4}	6.4×10
7	7.50×10^{-4}	6.76×10^{-8}	2.50×10^{-4}	8.5×10
8	1.00×10^{-3}	6.76×10^{-8}	2.50×10^{-4}	9.8×10
9	1.25×10^{-3}	6.76×10^{-8}	2.50×10^{-4}	1.13×10^2
10	2.50×10^{-4}	6.76×10^{-8}	1.00×10^{-3}	1.05×10

Conditions: 25 °C, 0.10 M NaTFA, $[\text{Ru}^{\text{III}}(\text{EDTA})(\text{pyam})^{2-}] = 1 \times 10^{-5} \text{ M}$; exps. 1–3 acetate buffer (10^{-2} M); exps. 4–10 phosphate buffer (10^{-2} M).

The derived rate law for this mechanism is given by

$$-\frac{d[\text{P}]}{[\text{P}_\infty] - [\text{P}]} = k_{\text{obsd}} \cdot dt \quad (4)$$

where $[\text{P}]$ and $[\text{P}_\infty]$ refer to the concentrations of the $[\text{Ru}^{\text{II}}(\text{EDTA})(\text{ampy})]^{2-}$ product at a variable time and at the end of the reaction, respectively. The observed rate constant is expressed by

$$k_{\text{obsd}} = \frac{k \cdot K_r \cdot K_{\text{OH}} [\text{Fe}^{\text{III}}] [\text{OH}^-]}{[\text{Fe}^{\text{II}}] + K_{\text{OH}} [\text{Fe}^{\text{II}}] [\text{OH}^-] + K_r K_{\text{OH}} [\text{Fe}^{\text{III}}] [\text{OH}^-]} \quad (5)$$

The reciprocal form of equation (5) is given by

$$\frac{1}{k_{\text{obsd}}} = \frac{1}{k} + \frac{[\text{Fe}^{\text{II}}]}{k K_r [\text{Fe}^{\text{III}}]} + \frac{[\text{Fe}^{\text{II}}]}{k K_r K_{\text{OH}} [\text{Fe}^{\text{III}}] [\text{OH}^-]} \quad (6)$$

Linear plots of k_{obsd}^{-1} against $[\text{Fe}^{\text{III}}]^{-1}$ and $[\text{OH}^-]^{-1}$ were observed in this work, as expressed by equations (7) and (8), in agreement with equation (6).

$$\frac{1}{k_{\text{obsd}}} = 4.4(\pm 0.2) \times 10^{-3} + 5.6(\pm 0.2) \times 10^{-6} / [\text{Fe}^{\text{III}}] \quad (7)$$

$$\frac{1}{k_{\text{obsd}}} = 2(\pm 2) \times 10^{-2} + 1.24(\pm 0.2) \times 10^{-9} / [\text{OH}^-] \quad (8)$$

The kinetic and equilibrium constants, k , K_r and K_{OH} , respectively, can be solved from the experimental and theoretical equations (6)–(8). In this way,

$$k = 227 \text{ s}^{-1}; K_r = 1.07 \text{ and } K_{\text{OH}} = 3.3 \times 10^6 \text{ M}^{-1}$$

The rate constant $k = 227 \text{ s}^{-1}$ is relatively small for a single intramolecular electron transfer reaction, and may

reflect an additional energy barrier, associated with the elimination of the methylene proton to form the diimine bond.

The equilibrium constant $K_r = 1.07$ implies that the redox potential for the intermediate ruthenium complex is very close to that for hexacyanoferrate (III)/(II) couple, i.e., 0.41 V vs SHE. This value coincides with the redox potential for the intermediate wave (2) shown in the cyclic voltammograms of Figure 2.B.

The basicity constant $K_{OH} = 3.3 \times 10^6 \text{ M}^{-1}$, is consistent with a pK_a of 7.48 for the deprotonation of the ampy ligand coordinated to the $[\text{Ru}^{\text{III}}(\text{EDTA})]^{2-}$ moiety. This value is smaller than that reported for the $[\text{Fe}^{\text{III}}(\text{CN})_4(\text{ampy})]^{3+}$ complex ($pK_a = 12.3$), but is higher than that estimated⁴ for the $[\text{Ru}(\text{bipy})_2(\text{ampy})]^{3+}$ complex ($pK_a = 2.4$). Therefore, the electron withdrawing power of the metal ion, which is responsible for the increase in the acidity of the coordinated ligands, vary in the order:



In conclusion, the electrochemical and kinetic results obtained in this work indicate that the oxidative dehydrogenation of the ampy ligand proceeds according to successive one electron transfer steps, with the involvement of Ru(III) intermediate species. The mechanism is quantitatively consistent with the kinetic data. For the first time, the kinetic constant for the intramolecular, metal-induced electron transfer step has been evaluated in this type of system.

Acknowledgement

We thank CNPq, FAPESP and FINEP for financial support.

References

REFERENCES

1. S. E. Diamond, G. M. Tom and H. Taube, *J. Am. Chem. Soc.* **97**, 2661-2664 (1975)
2. G. M. Brown, T. R. Weaver, F. R. Keene and T. J. Meyer, *Inorg. Chem.* **15**, 190-196 (1976)
3. H. E. Toma, A. M. C. Ferreira and N. Y. M. Iha, *Nouveau J. Chimie* **9**, 473-478 (1985).
4. M. J. Ridd and F. R. Keene, *J. Am. Chem. Soc.* **103**, 5733-5740 (1981).
5. A. M. C. Ferreira and H. E. Toma, *J. Chem. Soc. Dalton* 2051-2055 (1983).
6. H. E. Toma and E. Stadler, *Inorg. Chim. Acta* **119**, 49-53 (1986).
7. M. Goto, M. Takeshita, N. Kanda, T. Sakai and V. L. Goedken, *Inorg. Chem.* **24**, 582-587 (1985)
8. Y. Yoshino, M. Kasahara and M. Saito, *Polyhedron* **4**, 1019-1021 (1985).
9. H. Taube, *Electron transfer of complex ions in solution* (Acad. Press, New York, 1970), p. 73.
10. R. A. Sheldon and J. K. Kochi, *Metal-Catalyzed oxidations of organic compounds* (Acad. Press, New York, 1981).
11. M. Mukaida, H. Okuno and T. Ishimori, *Nippon Kagaku Sashhi* **86**, 589-593 (1965).
12. T. Matsubara and C. Creutz, *Inorg. Chem.* **18**, 1956-1966 (1979)
13. V. E. Alvarez, R. J. Allen, T. Matsubara and P. C. Ford, *J. Am. Chem. Soc.* **96**, 7686-7692 (1974).
14. F. Holmes and F. Jones, *J. Chem. Soc.* 2398-2400 (1960).